Check for updates

Geophysical Research Letters

RESEARCH LETTER
10.1029/2021GL093007

A Morphodynamic Model to Evaluate Long-Term Sandbar Rebuilding Using Controlled Floods in the Grand Canyon

Erich R. Mueller[1] **and Paul E. Grams**[2]

[1]Department of Physical Science, Geosciences Program, Southern Utah University, Cedar City, UT, USA, [2]U.S. Geological Survey, Southwest Biological Science Center, Grand Canyon Monitoring and Research Center, Flagstaff, AZ, USA

Key Points:

- A simple morphodynamic model using sub-daily flow and sediment concentration data predicts decadal changes in average sandbar volume
- The model optimizes an erosion rate parameter and eddy exchange coefficient and is relatively insensitive to the calibration data
- Post-hoc modeling demonstrates the importance of flood frequency and sand concentration for increasing average sandbar volume

Supporting Information:

Supporting Information may be found in the online version of this article.

Correspondence to:

E. R. Mueller,
erichmueller@suu.edu

Citation:

Mueller, E. R., & Grams, P. E. (2021). A morphodynamic model to evaluate long-term sandbar rebuilding using controlled floods in the Grand Canyon. *Geophysical Research Letters*, *48*, e2021GL093007. https://doi.org/10.1029/2021GL093007

Received 16 FEB 2021
Accepted 24 APR 2021

© 2021. American Geophysical Union. All Rights Reserved.

Abstract Controlled floods released from dams have become a common restoration strategy in river systems worldwide. Here we present a morphodynamic model of sandbar volume change for a subset of sandbars of the Colorado River in Grand Canyon National Park, where controlled floods are part of a management strategy focused on sandbar maintenance. We simulate sandbars as a triangular wedge, where deposition and erosion are modeled using physically based approaches that are driven by nearly continuous observations of flow and suspended sand concentration. We optimize an eddy exchange coefficient and erosion rate parameter by comparing model predictions to measured bar volumes. The model captures most of the variability in observed volume changes, and demonstrates the importance of flood frequency and sand concentration on average bar size. The model is easily implemented and adaptable, providing a means for predicting the future behavior of sandbars under a variety of streamflow and sediment supply scenarios.

Plain Language Summary Dams disrupt the natural streamflow and sediment supply regime of rivers. Downstream from dams, reduced flood magnitude often leads to channel simplification and reduced sediment supply may cause erosion of sediment deposits. River managers now use controlled floods—floods that mimic, but are typically smaller, than the natural pre-dam floods—to restore aspects of the natural river regime. The number of sandbars along the Colorado River in Grand Canyon National Park was reduced following the completion of Glen Canyon Dam, and eight controlled floods have been released since 1996. The floods effectively rebuild sandbars, but the sandbars often erode in the months following the floods. River managers thus need a modeling tool to evaluate the appropriate frequency of floods to sustain larger sandbars, while minimizing losses in hydropower generation from flow releases that exceed power plant capacity. Here we present a simple, physically based model to evaluate long-term (years to decades) effects of controlled floods on sandbar growth and decay. The model successfully reproduces the observed trends, and demonstrates the importance of more frequent floods to sustain sandbars in the river corridor.

1. Introduction

River canyons are some of the most dramatic features of Earth's surface. Within river canyons, alluvial sediments are confined to a narrow veneer along the channel bed and banks. While bedrock and coarse sediment such as boulders form the rigid channel boundary, fine sediments comprise a dynamic and transient part of the river corridor (e.g., Skalak & Pizzuto, 2010). Fine sediments provide substrate for riparian vegetation, morphological complexity for the aquatic ecosystem, protection of archeological resources, and important recreational areas for visitors (Butterfield et al., 2020; East et al., 2017; Grams et al., 2010; Kaplinski et al., 2005; Korman et al., 2004; Meshkova & Carling, 2012). In canyon rivers where flow is strongly affected by bedrock or relatively immobile talus, flow hydraulics are often dictated by these fixed obstructions (Alvarez et al., 2016; Rennie et al., 2018; Venditti et al., 2014; Wright & Kaplinski, 2011). As a result, locations of sediment deposition and bar formation are typically stationary, forming in zones of flow separation and reattachment associated with the obstruction (Lisle, 1986; Schmidt, 1990).

In the Colorado River basin of the western United States, river canyons are common and historically carried very high fine sediment loads (Schmidt, 2008). Extensive dam building in the 1960s led to dramatic changes to the flow and sediment transport characteristics of the river system. Downstream from dams, sandbars

have eroded because reduced peak discharge decreases the elevation to which sand deposition occurs, reduced sand supply limits sediment available for deposition (Topping et al., 2000), and dam operations such as hydropeaking often erode bars through a combination of seepage erosion and mass failure (Alvarez & Schmeeckle, 2013; Budhu & Gobin, 1994; Dexter & Cluer, 1999). Similar erosion of sandbars has been observed in other dam-affected river systems such as the Platte River (Alexander et al., 2018) and Mekong River (Gu et al., 2020), and sediment reduction of rivers worldwide is causing major changes in sedimentation processes from braided rivers (Surian, 2006) to deltas (Giosan et al., 2014). In the Marble Canyon and Grand Canyon segments of the Colorado River (hereafter, Grand Canyon), the effect of Glen Canyon Dam on downstream sandbars has been well documented (e.g., Hazel, Topping, et al., 2006; Mueller et al., 2018; Schmidt & Graf, 1990). Decades of experimentation and adaptive flow management have mitigated some of the conditions that caused rapid bar erosion during the initial decades of dam operations, and experimental controlled floods intended to rebuild sandbars have been released since 1996 (Grams et al., 2015).

Controlled floods are becoming more widely implemented worldwide to affect river geomorphology for a variety of management goals (Loire et al., 2021). In Grand Canyon, controlled floods for sandbar rebuilding are released when sand has accumulated in the river channel following tributary floods. During a controlled flood, suspended sand is advected into eddies where it falls from suspension in zones of lower flow velocity to form or augment sandbars near the flow separation and flow reattachment points. During periods between floods, bars typically erode. A primary management goal of controlled flooding is to increase the average size of sandbars, but floods come at the expense of lost revenue for hydropower generation. While annual surveys and remote cameras provide an assessment of changes in bar size (Grams et al., 2018; Hazel et al., 2008), models that predict long-term sandbar response to managed flow and sediment regimes are important management tools for evaluating water release scenarios. Previous modeling approaches have often focused on individual sandbars or short reaches (Nelson & McDonald, 1996; Wiele et al., 1996), with 2-d and 3-d modeling approaches accurately reproducing patterns of flow but typically overpredicting deposition rates (Logan et al., 2010; Sloff et al., 2012). For longer river segments, Wiele et al. (2007) coupled a 1-d sand routing model with a 2-d morphodynamic model to predict sand transport and storage, but the model was not specifically designed to predict sandbar response.

Multidimensional morphodynamic models include more physical details in the model equations, but they are typically limited in spatial and temporal applicability and are extremely sensitive to imprecisely known boundary conditions (Sloff et al., 2012). Further, a simple model to rapidly evaluate flow release and sediment supply scenarios over longer time scales would be useful to resource managers and stakeholders. Here we focus on predicting the average response of "dynamic" sandbars, based on classes of sandbars in different geomorphic settings that have been demonstrated to respond similarly to controlled floods and other dam releases (Mueller et al., 2018). We utilize nearly continuous measurements of flow and sand concentration to drive a simple morphodynamic model to predict long-term (decadal) sandbar volume using physically based sand deposition and erosion equations.

1.1. Study Area

The sandbars at the focus of this study are located in the Colorado River within Grand Canyon National Park, Arizona (Mueller et al., 2018; Figure S1). The river here is in a debris fan-affected canyon, where the longitudinal profile and reach-scale river hydraulics are strongly controlled by interactions with bouldery debris fans emanating from tributary basins (Howard & Dolan, 1981). Sandbars often form within these "fan-eddy complexes" where the debris fan forms an upstream pool, a rapid at the constriction point, and a downstream eddy where flow expands and recirculates (Schmidt and Rubin, 1995). In the pre-dam river, sandbars were more extensive and generally free of significant vegetation due to scouring by large floods. Today, vegetation has stabilized parts of many sandbars in wider sections of the canyon where sandbars are more common (Mueller et al., 2018). In narrow sections of the canyon, considered "critical reaches" because of the relative rarity of sandbars, sandbars are more likely to erode following floods and remain relatively vegetation free—these more dynamic, transient bars are the focus of this study.

Flow of the Colorado River in Grand Canyon is completely controlled by Glen Canyon Dam. All fine sediment delivered from the upper Colorado River basin is now trapped in the reservoir upstream of the dam, and sand supplied to the Colorado River downstream from the dam is provided only by tributaries. The

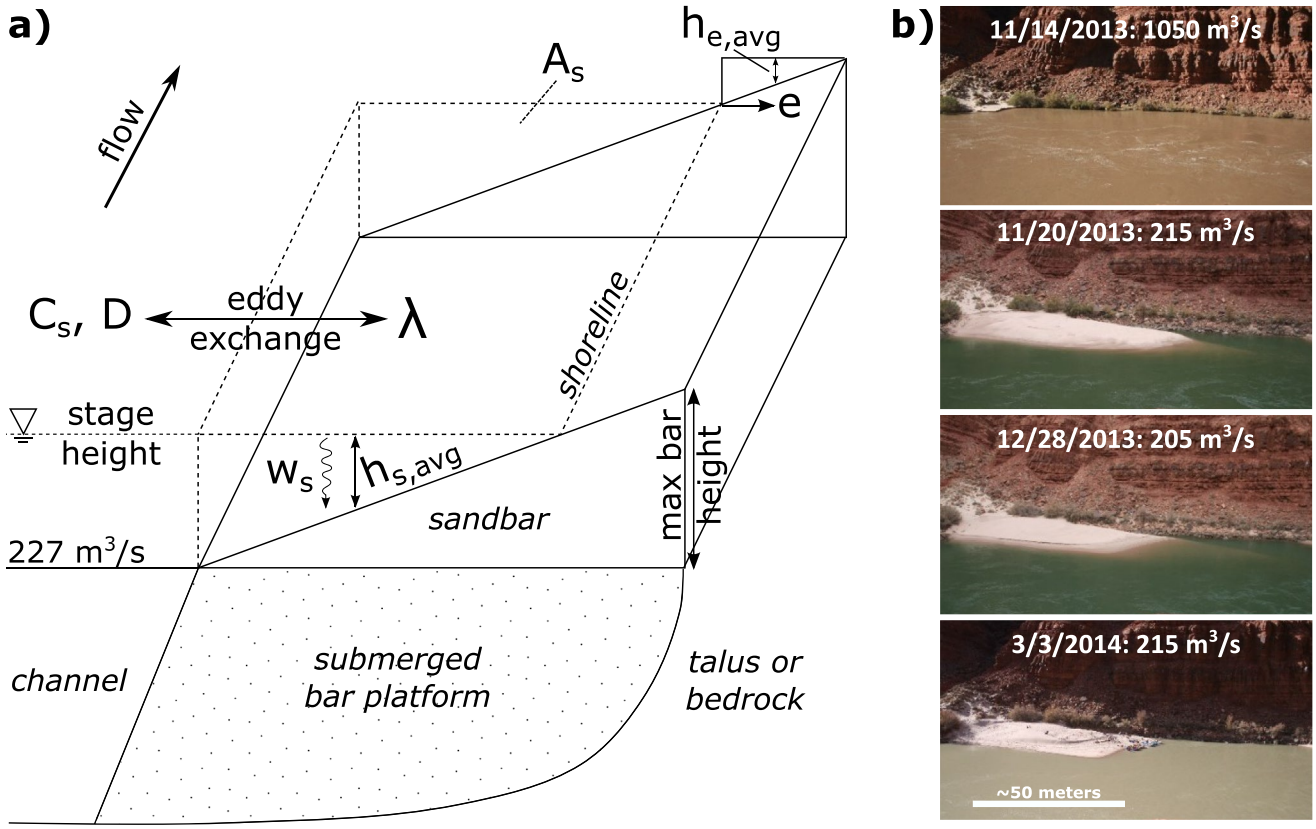

Figure 1. (a) Model schematic. All symbols for variables are described in the text. (b) Example sequence from bar submergence during a controlled flood (top panel) through four months of erosion of the bar that enlarged during the flood. Streamflow is from right to left.

Paria River, which enters 26 km downstream from the dam, is the dominant single supplier of sand to Grand Canyon and delivers approximately 5% of the pre-dam sand supply (Topping et al., 2000). The Paria River is largely unregulated and supplies significant quantities of sand most years during the North American Monsoon in the late summer and early fall. Since the implementation of a sediment-based flood protocol (Grams et al., 2015), large sand-supplying events from the Paria River triggered controlled floods in 2012, 2013, 2014, 2016, and 2018.

2. Methods

2.1. Modeling Approach

Our morphodynamic model builds on the eddy sand deposition model proposed by Andrews and Vincent (2007). Sandbars are represented as a triangular wedge (Figure 1), in which only part of the bar may be submerged, depending on the bar volume and stage elevation (depth) of flow. The model domain only includes the portion of the sandbar that is subaerially exposed during normal dam operations, which is the stage elevation associated with a discharge of 227 m^3/s, up to the maximum discharge of 1,274 m^3/s during controlled floods. Sand concentration and discharge in the main channel are assumed equal to values measured at the USGS gaging station (described below). In the model, sand is advected into the eddy using an eddy exchange coefficient, λ, which is the fraction of the eddy volume exchanged with the main channel per second (Andrews & Vincent, 2007). The volumetric flux of sand into the eddy, $Q_{s,i}$, is thus:

$$Q_{s,i} = \lambda C\left(A_s h_{s,\mathrm{avg}}\right), \quad (1)$$

where C is the vertically averaged sand concentration in the main channel, assumed to be uniform with depth for the purposes of the model. The quantity in parentheses is the eddy volume above the sandbar, where $h_{s,avg}$ is the average submergence depth over the bar and A_s is the submerged bar area based on the triangular bar geometry. We used the stage-discharge relation from a representative site to model depth (Hazel, Kaplinski, et al., 2006). From a mass balance perspective, $Q_{s,i}$ must be equal to the flux of sand out of the eddy plus the volumetric deposition of sand within the eddy (the sandbar):

$$\lambda C\left(A_s h_{s,\text{avg}}\right) = \lambda C_o\left(A_s h_{s,\text{avg}}\right) + w_s C_e A_s, \tag{2}$$

where C_o and C_e are the sand concentrations out of the eddy and within the eddy, respectively, and w_s is the settling velocity estimated using Dietrich (1982). Following Andrews and Vincent (2007), we use a linear approximation of C_e as the mean value of sand concentration into the eddy and out of the eddy. Solving for C_e in terms of C using this approximation, the volumetric deposition rate (right hand term in Equation 2), V_d, can be written as:

$$V_d = \frac{w_s \lambda h_{s,\text{avg}} C}{\frac{w_s}{2} + \lambda h_{s,\text{avg}}} A_s. \tag{3}$$

Mass failures and seepage-induced slumping are the most common mechanisms of sandbar erosion (Budhu & Gobin, 1994) and rates of erosion are highest following controlled floods when bars are larger (Dexter & Cluer, 1999; Hazel et al., 2010). We approximated these processes with two alternative approaches. First, we computed the volumetric erosion rate, E, by applying a constant, erosion rate parameter, e [L/T], along the length of shoreline, l, times the average exposed bar height, $h_{e,avg}$:

$$E = l h_{e,\text{avg}} e. \tag{4}$$

Thus, under this approach, no erosion occurs when the bar is fully submerged. Second, we use a simple exponential decay in volumetric erosion rate with bar volume:

$$E = e_2 Vol, \tag{5}$$

where Vol is the total bar volume and e_2 is the rate coefficient [1/T]. We did not consider aeolian processes that can also cause sediment redistribution on bars (Sankey et al., 2018).

Finally, we can calculate the sandbar volume change per time step by combining Equations 3 and 4 or 5 as:

$$\frac{dVol}{dt} = \frac{w_s \lambda h_{s,\text{avg}} C}{\frac{w_s}{2} + \lambda h_{s,\text{avg}}} \frac{A_s}{\left(1-\phi\right)} - E, \tag{6}$$

where ϕ is sediment porosity (assumed to be 0.35). Including sediment porosity converts volumetric deposition rates to an equivalent sandbar volume. We solve Equation 6 as a finite difference for each value in the time series of discharge and sediment concentration and update the volume. The three-dimensional triangular bar morphology is updated at each time step using an empirical volume-area relation derived from measurements at the study sites. See Text S1 for the full derivation.

2.2. Measured Sandbar Volume and Area

Forty-five sandbars have been measured annually to sub-annually since 1996 as part of a long-term monitoring program, reflecting a range in geomorphic settings and sandbar size (Hazel et al., 2008; Mueller et al., 2018, 2019). Topographic surveys made by field crews record changes in sandbar area and volume between the water level at a typical low flow (227 m^3/s) to an elevation corresponding to the maximum stage of controlled floods (1,274 m^3/s). For each survey, sand volume is computed as the volume above a constant reference surface within a common spatial footprint (Mueller et al., 2018). Most recent surveys occurred in September and October, whereas controlled floods are now typically released in November following sand inputs from the Paria River.

We selected a subset of nine of the 45 long-term monitoring bars for morphodynamic modeling (Tables S1 and S2). These are the most dynamic bars that lack dense vegetation cover, and where changes in sand storage dominantly occur in the eddy rather than main channel (the Group 1a bars of Mueller et al., 2018). Because these bars have limited vegetation cover, their growth and decay are controlled by physical processes more conducive to a simple physical model. The nine bars are dispersed throughout the canyon (Figure S1). Mueller et al. (2018) demonstrated that site geomorphology exerted a much stronger control on bar response to flow and sediment conditions than distance from the dam and we thus lumped these nine sites to model average bar response for sandbars in these types of geomorphic settings.

In order to capture the average response of the nine sandbars, regardless of total bar size, we normalized sand volume and area for each site by the maximum observed volume and area during the modeling period (2002–2019; 18 individual surveys) and calculated the mean normalized volume and standard error of the normalized volume for the nine sites. By normalizing each site in this way, it eliminates the disproportionate effect of large sandbars on the average condition - thus, we give each bar equal weight regardless of total bar volume. In order to convert the normalized bar volume (and area) to actual bar dimensions in order to calibrate the model for an "average bar", we multiply the normalized value by the average maximum volume of the modeled sites. The exact choice of bar normalization has relatively little effect on the model predictions.

2.3. Discharge and Suspended-Sand Concentration

Streamflow and suspended-sand concentration are available at 15-min increments for most of the study period, beginning in 2002. Suspended sand grain size data became available in 2007; prior to that date we assume a constant grain size equal to the average during the period of record. Suspended-sediment data are primarily derived from acoustic backscatter methods calibrated through traditional field methods (Topping & Wright, 2016). Here we present results using data from the USGS Colorado River near river mile 30 (09383050) stream gage, located 48 km downstream from the Paria River confluence.

2.4. Model Optimization

Equation 6 has two free parameters, the eddy exchange coefficient, λ, and erosion rate parameter, e or e_2, embedded in E. We implemented the model in Python, and optimized the free parameters using a Nelder-Mead approach in which the parameter space is searched using an iterative procedure to minimize the mean square error between the modeled and measured values (Evangelista et al., 2017; Nardi et al., 2013; Nelder & Mead, 1965).

2.5. Model Runs

We evaluated 11 versions of the model based on different calibration data sets, erosion models, and functions for λ (Table S3). In all calibration runs, the sand concentration and discharge are provided by observations (Figures 2a and 2b) and the sandbar volume was initialized to the volume measured in 2002. We evaluated constant (Const) λ and two versions in which λ increases with discharge as either a linear (Linear) or exponential (Exp) function (Text S1). In each case we applied both erosion models (E1, Equation 4; Eexp, Equation 5). To evaluate the sensitivity to the calibration, we varied the calibration data from just three observations (Range 3), selected to represent the range of measured volumes, to 10 values (Random 10), to all observations (Table S3).

3. Results and Discussion

The modeled long-term time series mimics the measured trend in sandbar volume closely and is relatively insensitive to the number of calibration points (Table S3, Figure 3); the five model runs in Figure 3 show a representative range in the model outcomes using different calibration data sets, erosion models, and functions for λ. Even when using only three observations for calibration, the results are very similar to those calibrated with the entire observational record (Table S3, Figure 3). This suggests that physical processes are reasonably well-represented by the model equations and that the flow and sediment boundary conditions

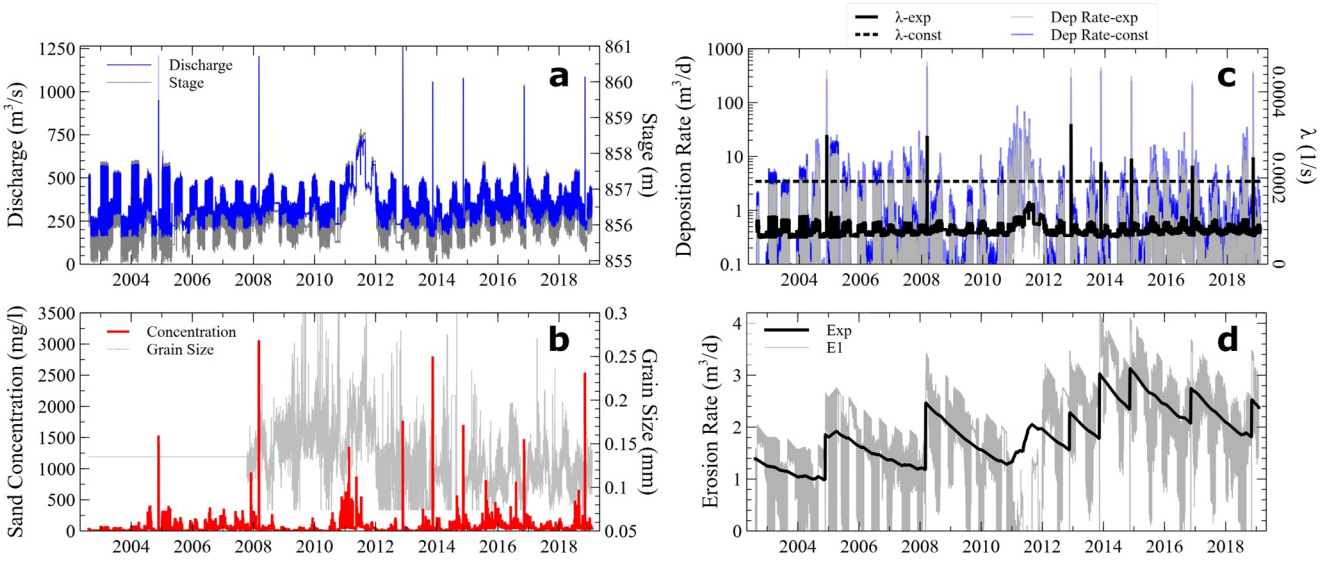

Figure 2. Time series of measured (a) discharge and stage and (b) sand concentration and grain size during the modeled period. Time series of modeled (c) variation in deposition rate for different λ models and (d) variation in erosion rate for different erosion models.

are well-defined. Figure 2c shows that sand deposition rates are strongly related to sand concentration and submerged bar depth. Bar deposition rates are lower between floods because much of the bar surface is not submerged. Bar deposition rates are much higher during floods because of the combination of high sediment concentrations and significant bar submergence. Erosion rates mimic total bar volume, but the erosion model using Equation 4 results in much more variable daily erosion rates (Figure 2d). Overall, the model successfully captures the peaks and troughs in the bar volume time series. Maximum bar volume is constrained by the accommodation space for sediment deposition as the bar grows to an upper limit. Minimum bar volume is constrained by diminishing erosion with shrinking bar size, which also increases the likelihood that lower flows will inundate the bar surface and deposit sediment. These modeled behaviors are consistent with field observations that bars do not necessarily reach a larger maximum size during floods just because they were initially larger, nor do bars disappear completely during long periods without floods.

The best-fit solutions had λ varying fivefold with discharge, indicating more intense exchange of flow with the main channel as discharge increases. In our model framework, this makes intuitive sense, in that the exchange between the main channel and eddy must be low near the minimum discharge and increase

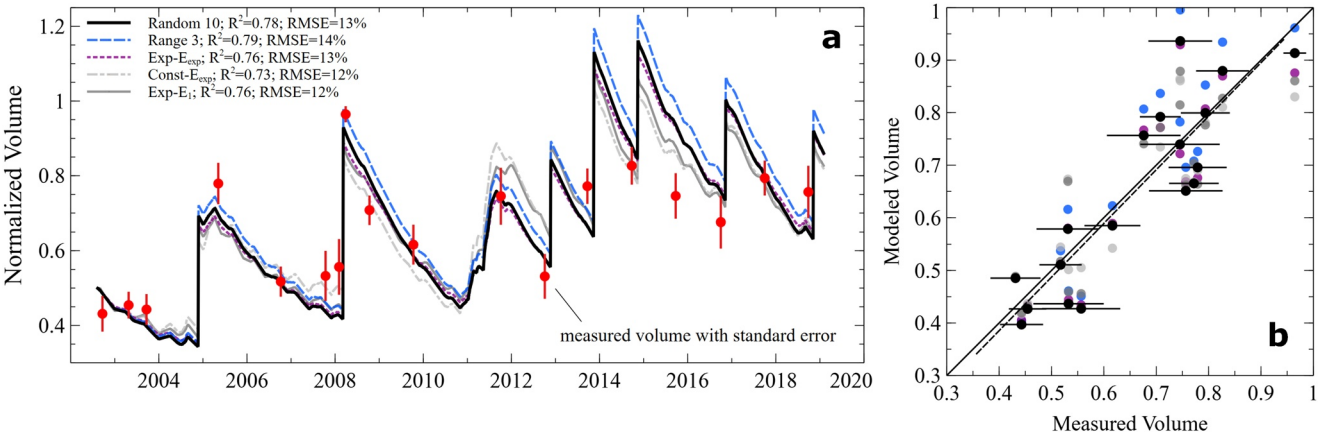

Figure 3. (a) Time series and (b) correlation of modeled versus measured bar volume for five of the model runs described in Table S3. The legend in (a) shows the R^2 and RMSE values (as a percent of the mean volume) for the indicated model runs.

as a proportion of the total flow as more of the bar is inundated. Further, the stage change is ~5 m from low to high flow, similar to our change in λ. Overall, our optimized values of λ are generally smaller than those measured in field settings by Andrews and Vincent (2007). In our case, the λ value has the effect of tuning the sand concentration measured at the USGS gaging station to the sand concentration in an eddy where flow velocity is likely less. Thus, the true concentration of sand at high elevation in the flow where deposition occurs in the model is likely less than the average sand concentration at the gaging station. One implication of this study is the need to better constrain the variability in λ, the relative concentration of sand in the channel versus the eddy, and the vertical profile of suspended sand concentration at a range of flows.

Of the two erosion models, the simple exponential decay approach (Equation 5) resulted in the best fit. The bank-line erosion model (Equation 4) led to more variable erosion rates, but did not improve model fit. In this approach, erosion behaves as exponential decay only for the proportion of the bar that is exposed above water level, causing rates to drop dramatically when the bar is intermittently submerged (Figure 2d). Dexter and Cluer (1999) note a more "gradual" long-term mode of erosion, compared to a more stochastic "event" mode. The event mode is variable and difficult to model, and thus it may be that the simple exponential decay model captures this gradual erosion reasonably well. Erosion rates predicted by the model ranged from roughly 0.04–4 m/d, within the range of 0.002–40 m/d measured by Dexter and Cluer (1999).

3.1. Post-Hoc Modeling of Flood Scenarios

An advantage of our model is the use of a simple physical framework with well constrained flow and sediment boundary conditions that allows for scenario modeling that is rapid and accessible to water managers and stakeholders. Because flow is constrained by operations of Glen Canyon Dam, and sediment supply is controlled by a few major tributaries, we expect boundary conditions and sandbar behavior during the calibration period to be representative of future conditions. The model can be applied as either a forecasting tool, in which synthetic hydrographs and predicted sediment concentration (Wright et al., 2010) are used to evaluate potential changes in sandbar volume, or as a "post-hoc" analysis tool to evaluate observed sandbar behavior relative to alternative dam operation scenarios.

Here, we evaluate the impact of controlled flood frequency since 2012 (Figure 4a) on predicted average sandbar volume using the "Random 10" (Figure 3) calibrated model. Five controlled floods have occurred during this time and there is some question about the cumulative benefit of individual floods and about differing flood magnitude, duration, or sediment scenarios. In this case, we "removed" floods from the sandbar model by smoothing the flow and sediment concentration record across the period when the controlled flood occurred. Under the observed protocol of frequent controlled floods, sandbars were almost twice as large as in the absence of floods. Bar volume was greater than 75% of maximum volume 50% of the time with frequent floods compared to no more than 40% of maximum volume 50% of the time without floods (Figure 4b). Each individual flood increases volume about 1.3–2 times the pre-flood volume such that more frequent controlled floods have an additive effect that increases average bar volume. When floods are less frequent, bars continue to erode, but eventually reach a minimum volume that varies slightly depending on seasonal changes in flow and sediment concentration (red line in Figure 4a).

The model can also be applied to evaluate how flood magnitude, duration, and sediment concentration affect sandbar response. Using the 2008 flood as an example, the model predicts steady deposition, with a slightly higher rate at the beginning of the event when sand concentration was higher (gray line in Figure 4c). Shortening or lengthening the flood by 30 h (~1/3) resulted in about a 15% corresponding decrease or increase in bar volume (Figure 4d). A reduction in magnitude of ~1/3, on the other hand, reduced post-flood bar volume by about 40%. Decreasing or increasing sand concentration by 25% affected predicted bar volume by about the same proportion as changes in flood duration (Figure 4e). These results suggest that sediment concentration and flood magnitude play comparable roles in the magnitude of sandbar deposition during floods (Schmidt, 1999; Topping et al., 2010).

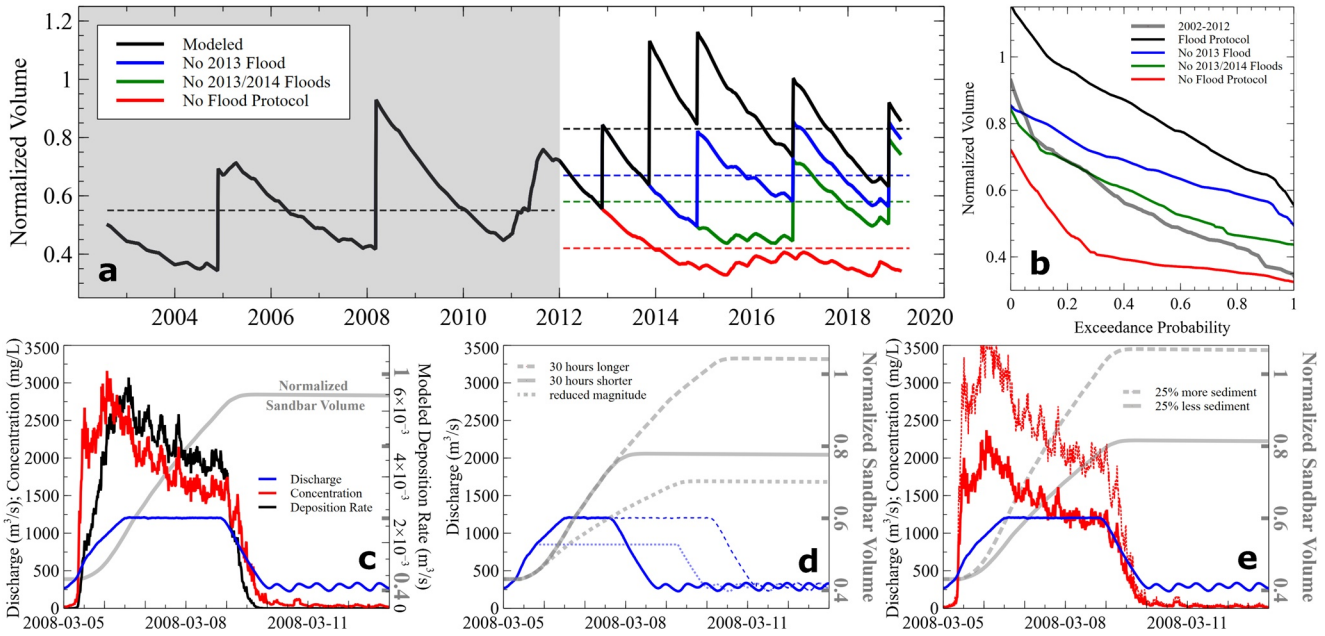

Figure 4. Sandbar scenario modeling. (a) Time series and (b) exceedance probability of bar volume for different frequencies of controlled floods during the period 2012–2019. Discharge, sand concentration, deposition rate, and normalized bar volume for (c) the 2008 controlled flood, (d) discharge and normalized bar volume during the 2008 flood with a 30 h increase in duration, and 30 h decrease in duration, and a 1/3 reduction in magnitude, and (e) discharge, sand concentration, and normalized bar volume the 2008 flood with 25% higher sand concentration and 25% lower sand concentration.

4. Conclusions

Controlled floods are routinely released to rebuild sandbars in Grand Canyon, and a model to predict sandbar dynamics to flow and sediment regimes is a valuable tool for evaluating different water release and sediment supply scenarios over both short and long time periods. Our model is parsimonious and process-based, and bar behavior is predicted accurately using the calibrated model. The quality of the data for flow and sediment boundary conditions combined with an abundance of observations for calibration allows for a simple modeling framework that captures the basic physics of the system. Sandbars are largest following controlled floods and decay toward a minimum size during normal dam operations. Post-hoc modeling demonstrates that significant increases in average sandbar volume occur with increasing frequency of controlled floods, and individual flood effectiveness depends roughly equally on the flood magnitude and sediment concentration during the flood. The model could be easily combined with economic models that incorporate hydropower generation or climate simulations of changes in water and sediment supply.

Data Availability Statement

Streamflow and sediment concentration data used in this study are available at https://www.gcmrc.gov/discharge_qw_sediment/. Sandbar volume data used in this study are available from two USGS data releases: https://doi.org/10.5066/P93F8JJK (Grams et al., 2020) and https://doi.org/10.5066/F7HD7SSW (Mueller et al., 2019).

Acknowledgments
We would like to thank the U.S. Department of Interior Bureau of Reclamation Glen Canyon Dam Adaptive Management Program for funding and support. Carl Legleiter and two anonymous reviewers provided important feedback on an earlier version of this manuscript. Any use of trade, product, or firm names is for descriptive purposes only and does not imply endorsement by the U.S. Government.

References

Alexander, J. S., Jorgensen, J. G., & Brown, M. B. (2018). Reproductive ecology of interior least tern and piping plover in relation to Platte River hydrology and sandbar dynamics. *Ecology and Evolution*, *8*(11), 5674–5679. https://doi.org/10.1002/ece3.4109

Alvarez, L. V., & Schmeeckle, M. W. (2013). Erosion of river sandbars by diurnal stage fluctuations in the Colorado River in the Marble and Grand Canyons: Full-scale laboratory experiments. *River Research and Applications*, *29*, 839–854. https://doi.org/10.1002/rra.2576

Alvarez, L. V., Schmeeckle, M. W., & Grams, P. E. (2016). A detached eddy simulation model for the study of lateral separation zones along a large canyon-bound river. *Journal of Geophysical Research: Earth Surface*, *122*(1), 25–49. https://doi.org/10.1002/2016JF003895

Andrews, E. D., & Vincent, K. R. (2007). Sand deposition in shoreline eddies along five wild and scenic rivers, Idaho. *River Research and Applications*, *23*(1), 7–20. https://doi.org/10.1002/rra.960

Budhu, M., & Gobin, R. (1994). Instability of sandbars in Grand Canyon. *Journal of Hydraulic Engineering*, *120*, 919–933. https://doi.org/10.1061/(asce)0733-9429(1994)120:8(919)

Butterfield, B. J., Grams, P. E., Durning, L. E., Hazel, J., Palmquist, E. C., Ralston, B. E., & Sankey, J. B. (2020). Associations between riparian plant morphological guilds and fluvial sediment dynamics along the regulated Colorado River in Grand Canyon. *River Research and Applications*, *36*(3), 410–421. https://doi.org/10.1002/rra.3589

Dexter, L. R., & Cluer, B. L. (1999). Cyclic erosional instability of sandbars along the Colorado River, Grand Canyon, Arizona. *Annals of the Association of American Geographers*, *89*(2), 238–266. https://doi.org/10.1111/1467-8306.00144

Dietrich, W. E. (1982). Settling velocity of natural particles. *Water Resources Research*, *18*(6), 1615–1626. https://doi.org/10.1029/wr018i006p01615

East, A. E., Sankey, J. B., Fairley, H. C., Caster, J. J., & Kasprak, A. (2017). *Modern landscape processes affecting archeological sites along the Colorado River corridor downstream of Glen Canyon Dam, Glen Canyon National Recreation Area, Arizona*. (U.S. Geological Survey Scientific Investigations Report 2017–5082). U.S. Geological Survey. https://doi.org/10.3133/sir20175082

Evangelista, S., Giovinco, G., & Kocaman, S. (2017). A multi-parameter calibration method for the numerical simulation of morphodynamic problems. *Journal of Hydrology and Hydromechanics*, *65*(2), 175–182. https://doi.org/10.1515/johh-2017-0014

Giosan, L., Syvitski, J., Constantinescu, S., & Day, J. (2014). Climate change: Protect the world's deltas. *Nature*, *516*(7529), 31–33. https://doi.org/10.1038/516031a

Grams, P. E., Hazel, J. E., Jr, Kaplinski, M., Ross, R. P., Hamill, D., Hensleigh, J., & Gushue, T. (2020). *Long-term sandbar monitoring data along the Colorado River in Marble and Grand Canyons, Arizona*. U.S. Geological Survey Data Release. https://doi.org/10.5066/P93F8JJK

Grams, P. E., Schmidt, J. C., & Andersen, M. E. (2010). *2008 high-flow experiment at Glen Canyon Dam—Morphologic response of eddy-deposited sandbars and associated aquatic backwater habitats along the Colorado River in Grand Canyon National Park*. (U.S. Geological Survey Open-File Report 2010–1032). U.S. Geological Survey. https://doi.org/10.3133/ofr20101032

Grams, P. E., Schmidt, J. C., Wright, S. A., Topping, D., Melis, T. S., & Rubin, D. M. (2015). Building sandbars in the Grand Canyon. *EOS Transactions of the American Geophysical Union*, *96*, 1–11. https://doi.org/10.1029/2015eo030349

Grams, P. E., Tusso, R. B., & Buscombe, D. (2018). *Automated Remote Cameras for Monitoring Alluvial Sandbars on the Colorado River in Grand Canyon, Arizona*. (U.S. Geological Survey Open-File Report 2018-1019). U.S. Geological Survey. https://doi.org/10.3133/ofr20181019

Gu, Z., Fan, H., & Wang, Y. (2020). Dynamic characteristics of sandbar evolution in the lower Lancang-Mekong River between 1993 and 2012 in the context of hydropower development. *Estuarine, Coastal and Shelf Science*, *237*, 106678. https://doi.org/10.1016/j.ecss.2020.106678

Hazel, J. E., Jr, Grams, P. E., Schmidt, J. C., & Kaplinski, M. (2010). *Sandbar response in Marble and Grand Canyons, Arizona, following the 2008 high-flow experiment on the Colorado River*. (U.S. Geological Survey Scientific Investigations Report 2010–5015). U.S. Geological Survey. https://doi.org/10.3133/sir20105015

Hazel, J. E., Jr, Kaplinski, M., Parnell, R., Kohl, K., & Schmidt, J. C. (2008). *Monitoring fine-grained sediment in the Colorado River Ecosystem, Arizona—Control network and conventional survey techniques*. (U.S. Geological Survey Open-File Report 2008-1276). U.S. Geological Survey. https://doi.org/10.3133/ofr20081276

Hazel, J. E., Jr, Kaplinski, M., Parnell, R., Kohl, K., & Topping, D. J. (2006). *Stage-discharge relations for the Colorado River in Glen, Marble, and Grand Canyons, Arizona, 1990-2005*. (U.S. Geological Survey Open-File Report 2006–1243). U.S. Geological Survey.

Hazel, J. E., Jr, Topping, D. J., Schmidt, J. C., & Kaplinski, M. (2006). Influence of a dam on fine-sediment storage in a canyon river. *Journal of Geophysical Research*, *111*, F01025. https://doi.org/10.1029/2004JF000193

Howard, A., & Dolan, R. (1981). Geomorphology of the Colorado River in the Grand Canyon. *The Journal of Geology*, *89*(3), 269–298. https://doi.org/10.1086/628592

Kaplinski, M., Behan, J., Hazel, J. E., Parnell, R. A., & Fairley, H. C. (2005). Recreational values and campsites in the Colorado River Ecosystem. In S. P. Gloss, J. E. Lovich, & T. S. Melis (Eds.), *The state of the Colorado River ecosystem in Grand Canyon, U.S. Geological Survey Circular 1282* (pp. 193–205). U.S. Geological Survey.

Korman, J., Wiele, S. M., & Torizzo, M. (2004). Modeling effects of discharge on habitat quality and dispersal of juvenile humpback chub (Gila cypha) in the Colorado River, Grand Canyon. *River Research and Applications*, *20*, 379–400. https://doi.org/10.1002/rra.749

Lisle, T. E. (1986). Stabilization of a gravel channel by large streamside obstructions and bedrock bends, Jacoby Creek, Northwestern California. *The Geological Society of America Bulletin*, *97*(8), 999–1011. https://doi.org/10.1130/0016-7606(1986)97<999:soagcb>2.0.co;2

Logan, B., Nelson, J., McDonald, R., & Wright, S. (2010). Mechanics and modeling of flow, sediment transport and morphologic change in riverine lateral separation zones. In *Proceedings of the 2nd Joint Federal Interagency Conference* (pp. 12).

Loire, R., Piégay, H., Malavoi, J.-R., Kondolf, G. M., & Bêche, L. A. (2021). From flushing flows to (eco)morphogenic releases: Evolving terminology, practice, and integration into river management. *Earth-Science Reviews*, *213*, 103475. https://doi.org/10.1016/j.earscirev.2020.103475

Meshkova, L. V., & Carling, P. A. (2012). The geomorphological characteristics of the Mekong River in northern Cambodia: A mixed bedrock-alluvial multi-channel network. *Geomorphology*, *147–148*, 2–17. https://doi.org/10.1016/j.geomorph.2011.06.041

Mueller, E. R., Grams, P. E., Hazel, J. E., Jr, & Schmidt, J. C. (2018). Variability in eddy sandbar dynamics during two decades of controlled flooding of the Colorado River in the Grand Canyon. *Sedimentary Geology*, *363*, 181–199. https://doi.org/10.1016/j.sedgeo.2017.11.007

Mueller, E. R., Hazel, J. E., Jr, Ross, R. P., & Grams, P. E. (2019). *Colorado River eddy sandbar dynamics data*. U.S. Geological Survey Data Release. https://doi.org/10.5066/F7HD7SSW

Nardi, L., Campo, L., & Rinaldi, M. (2013). Quantification of riverbank erosion and application in risk analysis. *Natural Hazards*, *69*(1), 869–887. https://doi.org/10.1007/s11069-013-0741-8

Nelder, J. A., & Mead, R. (1965). A simplex method for function minimization. *The Computer Journal*, *7*, 308–313. https://doi.org/10.1093/comjnl/7.4.308

Nelson, J. M., & McDonald, R. R. (1996). *Mechanics and modeling of flow and bed evolution in lateral separation eddies*. (Report to the Grand Canyon Monitoring and Research Center). U.S. Geological Survey.

Rennie, C. D., Church, M., & Venditti, J. G. (2018). Rock control of river geometry: The Fraser Canyons. *Journal of Geophysical Research: Earth Surface*, *123*(8), 1860–1878. https://doi.org/10.1029/2017jf004458

Sankey, J. B., Caster, J., Kasprak, A., & East, A. E. (2018). The response of source-bordering aeolian dunefields to sediment-supply changes 2: Controlled floods of the Colorado River in Grand Canyon, Arizona, USA. *Aeolian Research*, *32*, 154–169. https://doi.org/10.1016/j.aeolia.2018.02.004

Schmidt, J. C. (1990). Recirculating flow and sedimentation in the Colorado River in Grand Canyon, Arizona. *The Journal of Geology*, *98*, 709–724. https://doi.org/10.1086/629435

Schmidt, J. C. (1999). Summary and synthesis of geomorphic studies conducted during the 1996 controlled flood in Grand Canyon. In R. H. Webb, J. C. Schmidt, G. R. Marzolf, & R. A. Valdez (Eds.), *The controlled flood in Grand Canyon, American Geophysical Union Geophysical monograph series 110* (pp. 329–341). American Geophysical Union. https://doi.org/10.1029/gm110p0329

Schmidt, J. C. (2008). The Colorado River. In A. Gupta (Ed.), *Large rivers: Geomorphology and management* (pp. 183–224). John Wiley & Sons.

Schmidt, J. C., & Graf, J. B. (1990). *Aggradation and degradation of alluvial sand deposits, 1965 to 1986, Colorado River, Grand Canyon National Park, Arizona*. (U.S. Geological Survey Professional Paper 1493). U.S. Geological Survey. https://doi.org/10.3133/pp1493

Schmidt, J. C., & Rubin, D. M. (1995). Regulated streamflow, fine-grained deposits, and effective discharge in canyons with abundant debris fans. In J. E. Costa, A. J. Miller, K. W. Potter, & P. R. Wilcock (Eds.), *Natural and anthropogenic influences in fluvial geomorphology, American Geophysical Union Geophysical monograph series 89* (pp. 177–195). American Geophysical Union. https://doi.org/10.1029/gm089p0177

Skalak, K., & Pizzuto, J. (2010). The distribution and residence time of suspended sediment stored within the channel margins of a gravel-bed bedrock river. *Earth Surface Processes and Landforms*, *35*(4), 435–446.

Sloff, K., Nieuwboer, B., Logan, B., & Nelson, J. M. (2012). Effect of sediment entrainment and avalanching on modeling of Grand Canyon eddy bars. In R. M. Muñoz (Ed.), *River flow 2012: Proceeding of the international conference of fluvial hydraulics* (pp. 791–798). CRC Press.

Surian, N. (2006). Effects of human impact on braided river morphology: Examples from Northern Italy. In G. H. Sambrook Smith, J. L. Best, C. Bristow, & G. E. Petts (Eds.), Braided rivers: Process, deposits, ecology and management (Vol. 36, pp. 327–338). Wiley-Blackwell. International Association of Sedimentologists Special Publication

Topping, D. J., Rubin, D. M., Grams, P. E., Griffiths, R. E., Sabol, T. A., Voichick, N., et al. (2010). *Sediment transport during three controlled-flood experiments on the Colorado River downstream from Glen Canyon dam, with implications for eddy-sandbar deposition in Grand Canyon National Park*. (U.S. Geological Survey Open-File Report 2010–1128). U.S. Geological Survey. https://doi.org/10.3133/ofr20101128

Topping, D. J., Rubin, D. M., Vierra, L. E., Jr, & (2000). Colorado River sediment transport: 1. Natural sediment supply limitation and the influence of Glen Canyon Dam. *Water Resources Research*, *36*, 515–542. https://doi.org/10.1029/1999wr900285

Topping, D. J., & Wright, S. A. (2016). *Long-term continuous acoustical suspended-sediment measurements in rivers—Theory, application, bias, and error*. (U.S. Geological Survey Professional Paper 1823). U.S. Geological Survey. https://doi.org/10.3133/pp1823

Venditti, J. G., Rennie, C. D., Bomhof, J., Bradley, R. W., Little, M., & Church, M. (2014). Flow in bedrock canyons. *Nature*, *513*(7519), 534–537. https://doi.org/10.1038/nature13779

Wiele, S. M., Graf, J. B., & Smith, J. D. (1996). Sand deposition in the Colorado River in the Grand Canyon from flooding of the Little Colorado River. *Water Resources Research*, *32*, 3579–3596. https://doi.org/10.1029/96wr02842

Wiele, S. M., Wilcock, P. R., & Grams, P. E. (2007). Reach-averaged sediment routing model of a canyon river. *Water Resources Research*, *43*, W02425. https://doi.org/10.1029/2005WR004824

Wright, S. A., & Kaplinski, M. (2011). Flow structures and sandbar dynamics in a canyon river during a controlled flood, Colorado River, Arizona. *Journal of Geophysical Research*, *116*. https://doi.org/10.1029/2009JF001442

Wright, S. A., Topping, D. J., Rubin, D. M., & Melis, T. S. (2010). An approach for modeling sediment budgets in supply-limited rivers. *Water Resources Research*, *46*, W10538. https://doi.org/10.1029/2009WR008600